

New MEMS Microspectrometer for Infrared Absorption Spectroscopy

Martin Ebermann, Norbert Neumann

InfraTec GmbH, Gostritzer Strasse 61-63, 01217 Dresden, Germany

Abstract

In this paper we present basic designs, operation concepts and some application examples of a novel microspectrometer for the spectral range of 3-5 μm , which is based on a pyroelectric detector with an integrated micromachined Fabry-Perot filter (FPF). We discuss the influence of different optical setups on the spectral resolution and the signal-to-noise ratio of the microspectrometer. Two basic operation modes, step-scan mode and continuous-sweep mode are demonstrated. Such a device has a large potential in the field of infrared absorption spectroscopy, particularly if multicomponent mixtures have to be analyzed.

Introduction

Infrared absorption spectroscopy is well established in gas analysis, fire and flame detection and in many other applications. A typical infrared analyzer consists of a broadband light source, a sample cell and at least one but in most cases several spectral measurement channels with fixed narrow bandpass filters. The filters are selected to match the characteristic absorption bands that are of interest in each specific application. This is often realized by using detectors with several spectral channels or a rotating filter wheel in front of a single channel detector.

The increasing demand in collecting more and more spectral information, reducing cross sensitivities, making measurements faster and last but not least in miniaturization of such systems is challenging. The above mentioned conventional approach mainly suffers from the disadvantage, that the number of channels is limited. There are several well known problems, for example regarding a homogeneous detector illumination and long-term stability. Filter wheels cannot be miniaturized and their reliability is not sufficient.

What in fact is needed is a low resolving, robust and low cost microspectrometer for the mid-wave infrared range. Many approaches for microspectrometers are based on diffraction gratings [1]. Attempts to miniaturize the FTIR technique have also been reported [2]. Some of these solutions offer a relatively high spectral resolution and fast measurements, but the degree of integration and miniaturization is often not very high.

Many attempts towards the combination of a Fabry-Perot interferometer and an IR-detector have also been reported [3, 4, 5], but in most cases they suffer from a low Finesse due to warping of thin membrane reflectors or low optical throughput.

Our approach, the hybrid assembly of a bulk micromachined Fabry-Perot Filter (FPF) and a pyroelectric detector, results in a very compact spectrometer module [6]. Existing instrument designs can be easily adapted to the new tunable detector. In this paper we present the basic design and operation concept of such a microspectrometer for the spectral range of 3-5 μm .

Tunable detector

FABRY-PEROT INTERFEROMETER FUNDAMENTALS

The tunable detector is based on the well-known Fabry-Perot Interferometer (FPI), schematically shown in Fig. 1. Two flat and partially transmitting mirrors with reflectance R are arranged in parallel at a distance d , forming an optical gap characterized by the refractive index n . Multiple-beam interference is created inside the gap and thus only radiation can be transmitted, which satisfies the resonance condition according to equation (1). One of the mirrors is suspended by springs so that the distance d can be decreased by applying a control voltage. As the resonance condition changes; so does the wavelength of the transmitted radiation, neglecting the phase at reflection ϕ .

$$\lambda_m = \frac{2 n d \cos \beta}{m} \quad (1)$$

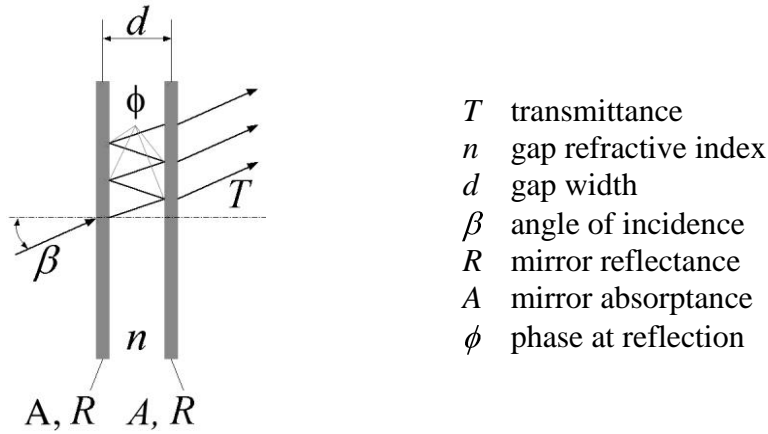


Fig. 1: Schematic of the FPI arrangement

The transmittance spectrum $T(\lambda)$ of a FPI is described by the Airy-Function (Fig. 2 & eq. 2). The center wavelength (*CWL*) of the filter corresponds to the resonant wavelength. In our case the first interference order ($m=1$) is used while the higher orders are blocked by means of an additional bandpass filter.

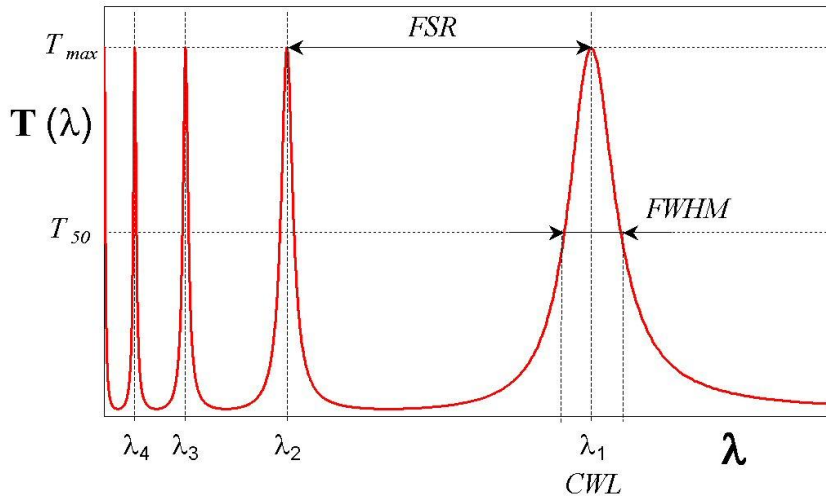


Fig. 2: Airy-function over wavelength

$$T = \left(1 - \frac{A}{1-R}\right)^2 \frac{1}{1 + \frac{4R}{(1-R)^2} \sin^2\left(2\pi d \frac{1}{\lambda} \cos\beta - \phi\right)} \quad (2)$$

The spectral bandwidth (*FWHM*) is the decisive factor regarding the spectral resolution of a FPI-based spectrometer (eq. 3).

$$FWHM \approx 2d \left(\frac{1-R}{\pi\sqrt{R}}\right) \quad (3)$$

The spectral distance of two adjacent interference peaks limits the maximum usable tuning range. This is denoted as the free spectral range (*FSR*). The ratio of the tuning range to the bandwidth (in the wavenumber domain) is given as the Finesse (F_{+R}), which is the figure of merit of a Fabry-Perot interferometer (eq. 4).

$$\tilde{F}_R = \frac{FSR}{FWHM} = \frac{\pi\sqrt{R}}{1-R} \quad (4)$$

DESIGN AND FABRICATION

In order to achieve the tuning of the resonator cavity, an electrostatic actuation using a parallel plate design has been chosen. It fits very well the filter set-up and can be easily integrated. The design principle of the bulk micromachined filter is shown in figure 3. It is based on a approach using relatively thick reflector carriers, one of them being fixed and the other suspended by springs which allow the movement in vertical direction. The stiffness of the thick reflector carriers allows us to realize a large aperture of 1.9 mm and a Finesse of 40 up to 60.

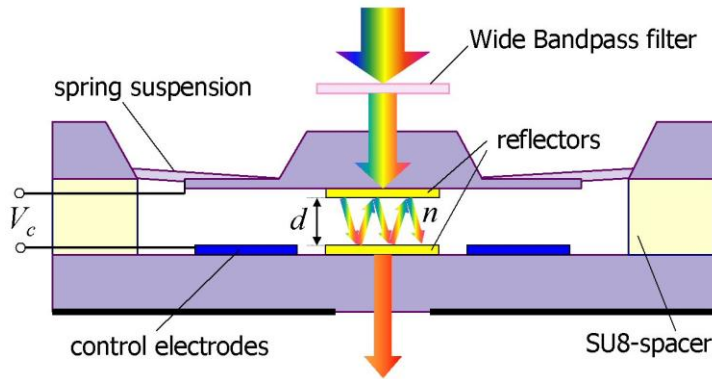


Fig. 3: Schematic cross-section of the MOEMS FPF

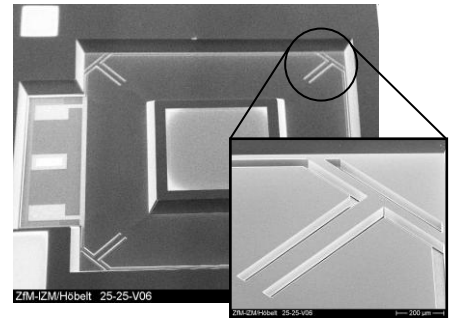


Fig. 4: Stress compensating springs

A set-up of coated and etched wafers is bonded directly or by an intermediate SU-8 layer. 300 µm thick silicon wafers with a resistivity of 5...10 Ωcm are used as carriers for both the fixed and the movable reflector. The fixed reflector is located in the center surrounded by the driving electrodes. The movable reflector is suspended by diagonally arranged springs located in the corners of the outer frame, shown in figure 4. The T-shape facilitates the reception of tensions in lengthwise direction, as the small T side can be bended crosswise. Advantages of this modification are the simple and proven technology, a large freedom of the design parameters and the high precision of the fabricated springs [6].

The filter is actuated electrostatically. Applying a tuning voltage V_c at the control electrodes with the area A_{el} results in an electrostatic force F_{el} decreasing the electrode gap d_{el} . (eq. 5). In the case of steady state, the typical non-linear characteristic tuning curve shown in figure 5 is produced.

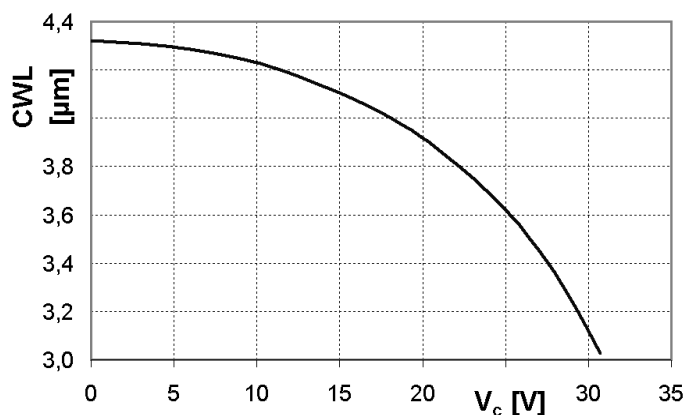


Fig. 5: Typical steady-state control characteristics

$$F_{el} = \frac{\epsilon_0 A_{el} V_c^2}{2d_{el}^2} \quad (5)$$

Distributed Bragg reflectors are commonly used to generate a broadband reflector. Bragg reflectors are built up by alternating quarter wave optical thickness (QWOT) layers with low and high refractive index. In order to generate a broad high reflective zone even with a low stack number, thin films with as high as possible refractive index ratio n_H/n_L have to be applied. Silicon dioxide with a refractive index of 1.38 at 4 μm and polycrystalline silicon with a refractive index of 3.33 at 4 μm is used for the reflectors. Because of the high refractive index ratio n_H/n_L of 2.41 wide high-reflective zones with a high average and maximum reflectance of about 95% and of 96 % respectively was obtained already with a $|\text{LH}|^2$ layer stack. Hence a double-stack $|\text{LH}|^2$ was chosen as Bragg reflector and the spectral range of 3...5 μm was divided in two sub-ranges with each 1100 nm from 3.0...4.1 μm und 3.9...5.0 μm . In figure 6 the reflectance is plotted for the short and long cavity filter versus wavelength.

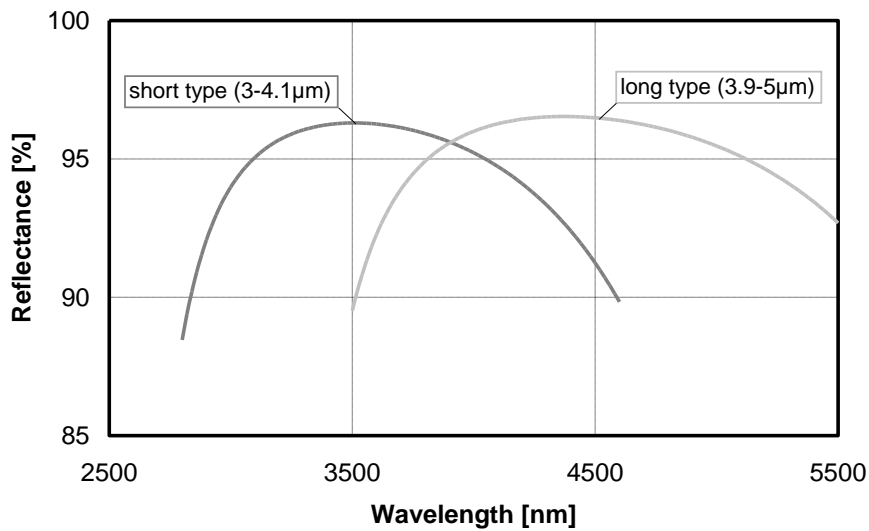


Fig. 6: Reflectance of $\text{SiO}_2/\text{Poly-Si } |\text{LH}|^2$ bragg reflectors for a spectral range of 3-4.1 μm and 3.9-5 μm

The backsides of the wafer were anti-reflection coated to reduce reflection losses and ripples in the high reflective band caused by multiple reflections in the silicon substrate. An often used double-layer design was refined to use only silicon dioxide and polycrystalline silicon layers for the ARC too, resulting in a triple-layer design. For the first layer a QWOT silicon dioxide layer with n_1 of 1.38 was chosen. The second layer was synthesized with very thin films of silicon dioxide and polycrystalline silicon to obtain a refractive index of about 2.3. The refined triple-layer ARC has an average reflectance of 0.6% in the hole spectral range of 3...5 μm and a minimum of 0.3%. In figure 7 the broadband triple-layer ARC is compared with single-layer ARC.

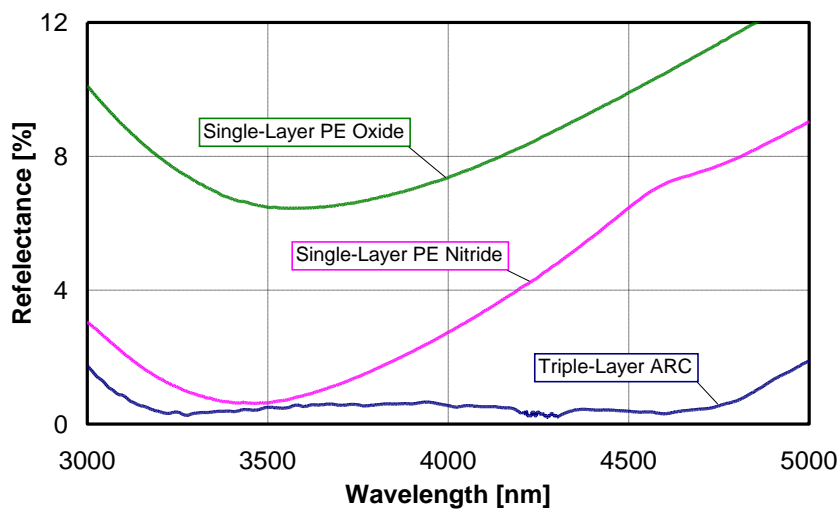


Fig. 7: Reflectance of single and triple-layer anti-reflection coating

SPECTRAL PERFORMANCE

Two types of FP-Filters have been realized, each covering a portion of the entire wavelength range from 3-5 μm . Performance data listed in the table 1 are typical values, which are achievable in series production. Tuning the *CWL* of the FPF results in a variation of the *FWHM* and the peak transmission within certain limits. The additionally wide band pass filter and the pyroelectric detector element show some spectral characteristics too. The spectral response of the detector is therefore a combination of different factors, but has to be considered as a whole in the application. It is stated as the relative spectral response, referring to a 'black' reference detector with a flat spectral response (see Fig. 8).

	short type	long type
Tuning range	3...4.1 μm	3.9...5 μm
FWHM	80 \pm 20nm	100 \pm 20nm
Peak-Transmittance	> 50 %	
Out-of-band blocking	< 0.5 %	
Finesse	40...60	

Table 1: Spectral performance data; measured with FTIR spectrometer, 8 cm^{-1} , $\pm 4^\circ$ div. angle

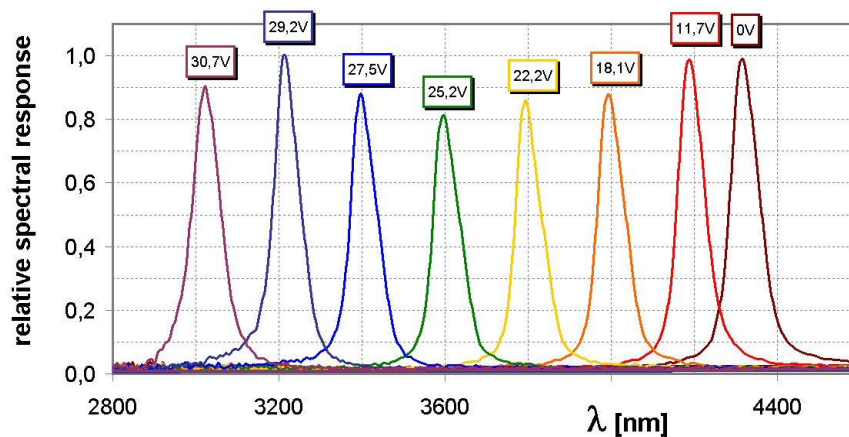


Fig. 8: Spectral response of a short type FP-detector at several tuning voltages; FTIR, 8 cm^{-1} , $\pm 4^\circ$ div. angle

PYROELECTRIC DETECTOR

The built-in LiTaO₃-based pyroelectric detector is a state of the art thermally compensated current-mode type with an integrated low-power and low-noise CMOS Op-Amp. It exhibits high specific detectivity and a flat frequency response up to several tens of Hz. The element size is 2x2mm². The high impedance circuit of the detector trans-impedance amplifier has to be protected from cross-talk caused by the FPF driving voltage. Therefore; an electrical shielding is implemented in the detector assembly. A special mounting technology prevents the FP-filter from warping due to mechanical stress.

	without FP-filter	FP-filter included
Frequency response	flat up to 40Hz	
Noise [$\mu\text{V}/\text{Hz}^{1/2}$]	65	
Responsivity R_v [kV/W]	120	2.5
Detectivity D* [$\text{cm Hz}^{1/2}/\text{W}$]	3.7·10 ⁸	7.7·10 ⁶

Table 2: Detector performance; 400°C blackbody, 10Hz; responsivity attenuation with FP-filter \approx 2%

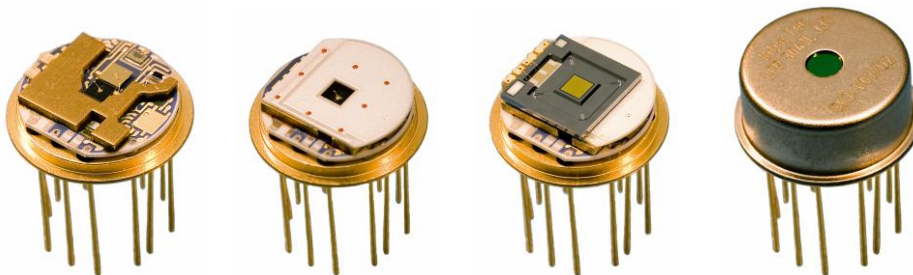


Fig. 9: Stages of the detector assembly

Spectrometer Design

The concept of a FPF-based microspectrometer is basically very simple and naturally similar to conventional NDIR-analyzers. It incorporates an infrared source, which is preferably electrically modulated, a sample cell, the tunable detector and a control unit. Nevertheless, some specific issues regarding the proper choice of the IR-source and the optical set-up need to be considered.

There is a trade off between the optical throughput, with it the signal-to-noise ratio SNR, and the spectral resolution, a principle, which is in fact valid for all spectrometric applications [9]. In the case of the FP-detector this is associated with the problem of collimation or divergence angle of detector illumination. A collimated but oblique incident beam causes a negative drift of the CWL (see Fig. 10 left). The most common case is an uncollimated beam with a certain angle of divergence and intensity profile. The resulting transmittance spectrum can be seen as the superposition of collimated ray-beams with different angles of incidence and intensities. It has a broader FWHM and the CWL at slightly lower wavelengths (see figure 10 right).

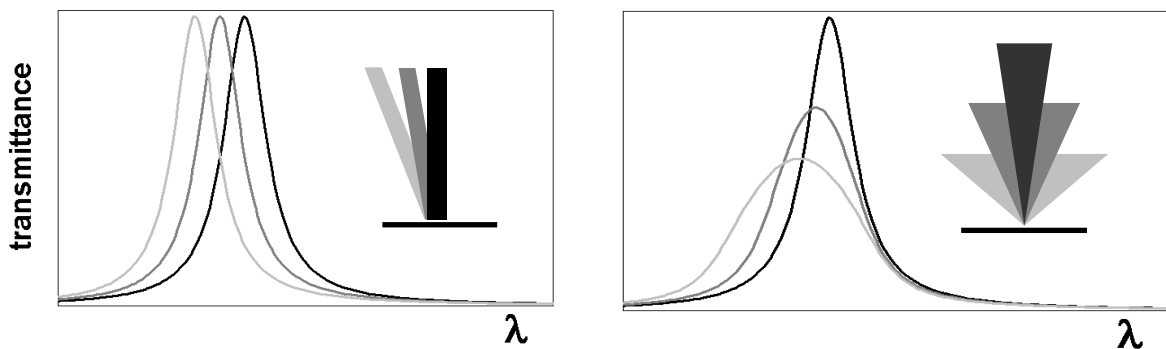


Fig. 10: Influence of angle shift and divergence angle on bandwidth and peak transmittance of a FPF

Beam divergence can be minimized by using a light source with collimated output or by means of an additional prefixed aperture (Fig. 11 left). If the desire is to maximize the optical throughput, then focusing optics can be used, but larger divergence angles will be a side effect (Fig. 11 right).

Obviously a compromise between spectral resolution and signal-to-noise ratio (SNR) needs to be found for each particular application.

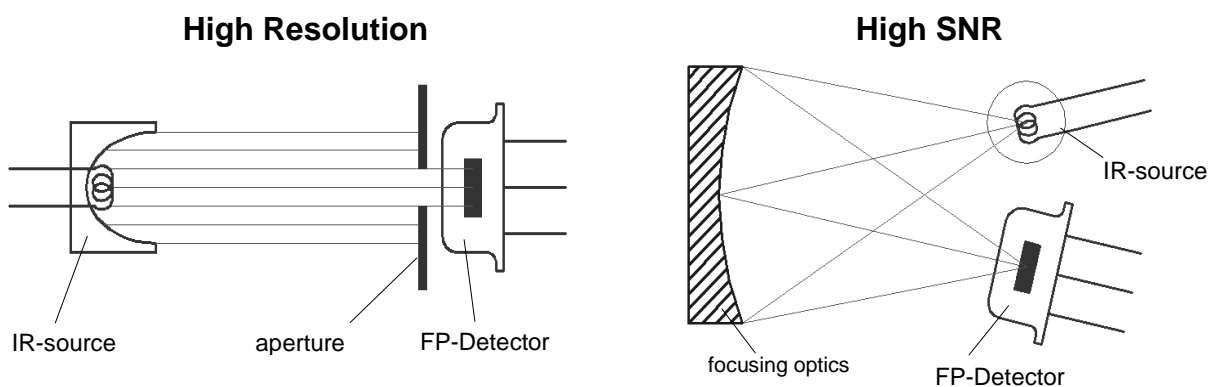


Fig. 11: Possible optimizations for the optical design of a microspectrometer with FPF detector

Figure 12 shows the correlation of the achievable SNR with a given spectral resolution, measured with two tested measurement setups according to figure 11. Please note that a parallel beam with a diameter of 1 mm offers the highest spectral resolution but only 3 % of the intensity and thus the resulting low detector signal voltage compared to an illumination using f/1.4 optics.

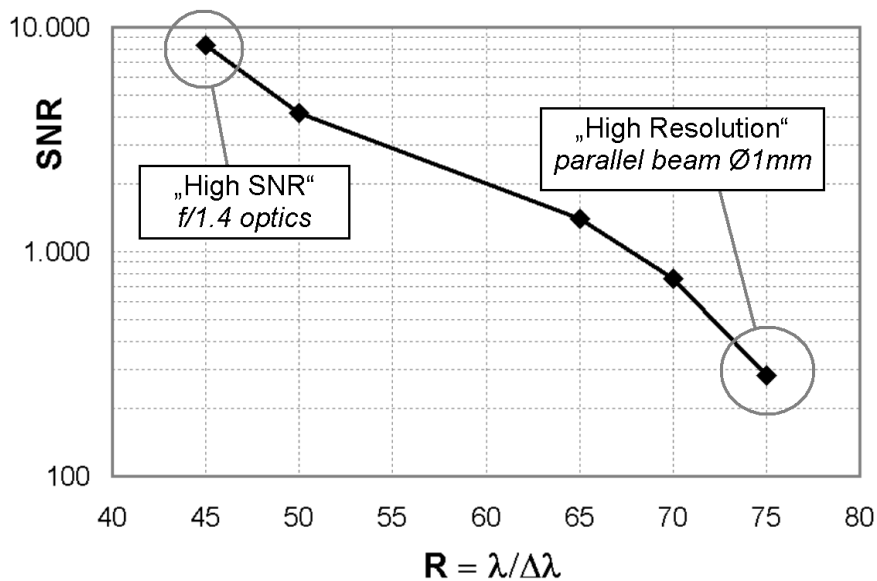


Fig 12: SNR vs. spectral resolution LFP-3041-337 with a modulated IR source

Spectrometer Operation

The capabilities of a tunable detector are numerous. Depending on the measurement task and operation mode, different advantages compared to conventional single or multi channel detectors with fixed NBP filters can be found. Two basic operation modes shall be explained in detail:

Step scan mode

This method is the very same as applied for conventional detectors, using a modulated light source and Lock-In or FFT algorithms. In addition to this we now switch the filter wavelength between the measurement points until we get the whole spectrum. The required acquisition time for the mapping of a spectrum depends on wavelength range and step size on one hand side and on modulation frequency and integration time to achieve the desired SNR on the other.

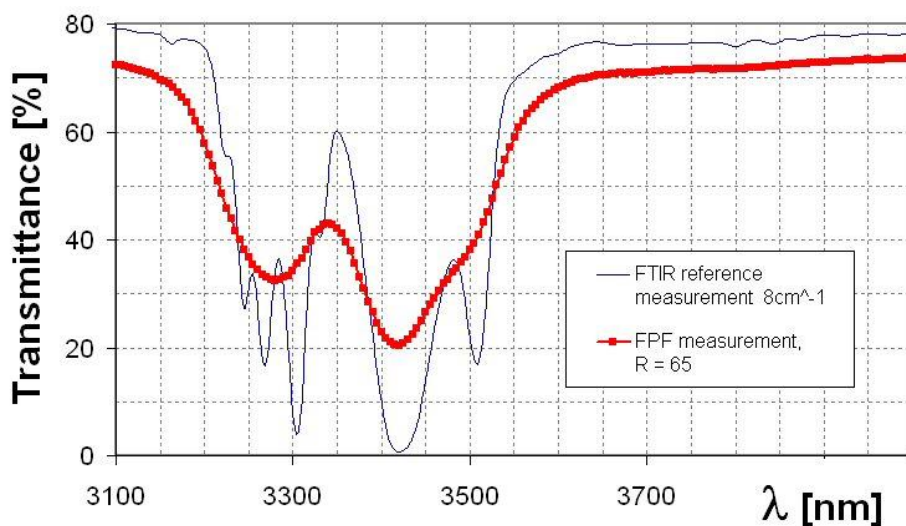


Fig 13: Step-Scan measurement of a polystyrene foil

Figure 13 gives an example for the step scan operation. The IR source (Intex MIRL17-900 reflector 900mW) is modulated with 10 Hz, while the filter is scanning the desired wavelength range from 3000-4000 nm at 100 steps (step size 10 nm). The acquisition of the spectrum needs 20 s. The achieved spectral resolution $\lambda/\Delta\lambda$ is about 65 and the signal-to-noise ratio about 1300:1.

Continuous sweep mode

By using a pyroelectric detector only modulated radiation can be analyzed. Normally this is realized by mechanical chopping or electrical modulation of the IR source. If the filter is, however, continuously swept the spectral information can be used directly for the modulation. The filter is actuated dynamically in this case. This particular operation mode has principally the potential to accelerate the recordings of spectra remarkably. The non-linear effects during dynamic operation, however, need to be considered separately.

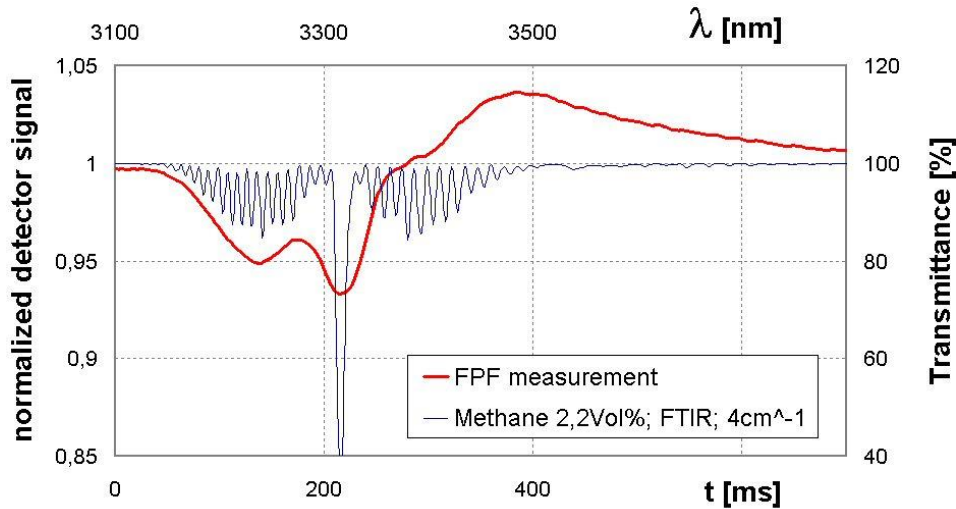


Fig 14: Measurement example for the continuous scan mode with dynamic filter tuning (2.2 vol% methane)

Figure 14 gives an example for the continuous sweep mode. The IR source is working in DC operation, while the filter goes through the desired wavelength range. Except for the DC portion, the whole spectral information is contained in the generated detector signal. The actuation and analysis has to include both the dynamic properties of the filter and the detector.

There is a large field of applications where speed is much more important than accuracy. One example could be the detection of a thin oil film on a steel substrate, another the assorting of polymer fractions. Often it is sufficient to detect the presence of a certain absorption band and to compare with one or two neighbored reference wavelength. With our tunable detector this can be solved by fast switching or sinusoidal modulating the filter wavelength. Figure 15 shows such an exemplary solution. The control voltage of the filter (dashed curve) is modulated in such a way, that the filter wavelength varies between $3,8\mu\text{m}$ and $3,0\mu\text{m}$ within 50ms. Without any sample in the optical path, the detector gives only a small signal (baseline, dotted curve). When inserting the sample (PE-LD foil, $10\mu\text{m}$) in the path strong absorption peaks appear in the signal (solid curve) that correspond to the absorption line of the PE-LD sample around $3,4\mu\text{m}$.

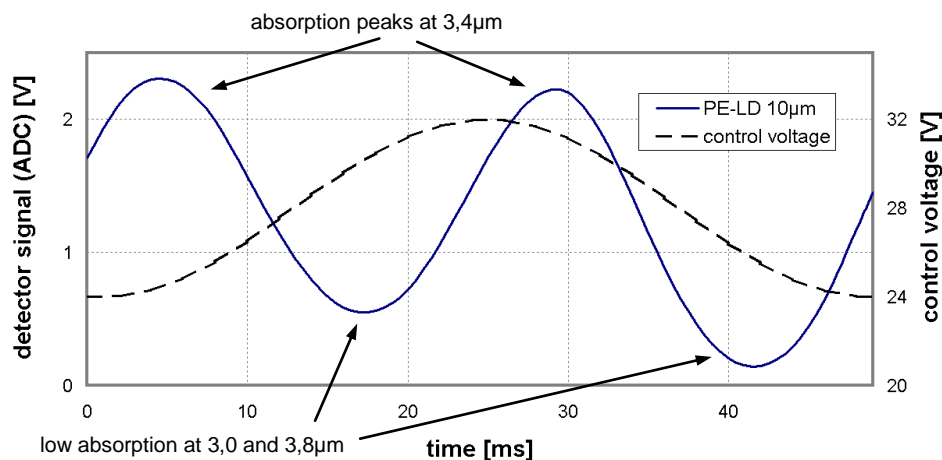


Fig 15: Fast sweep measurement example; PE-LD foil $10\mu\text{m}$
IR-source Intex M1RL17-900 800mW DC; tuning frequency 20Hz

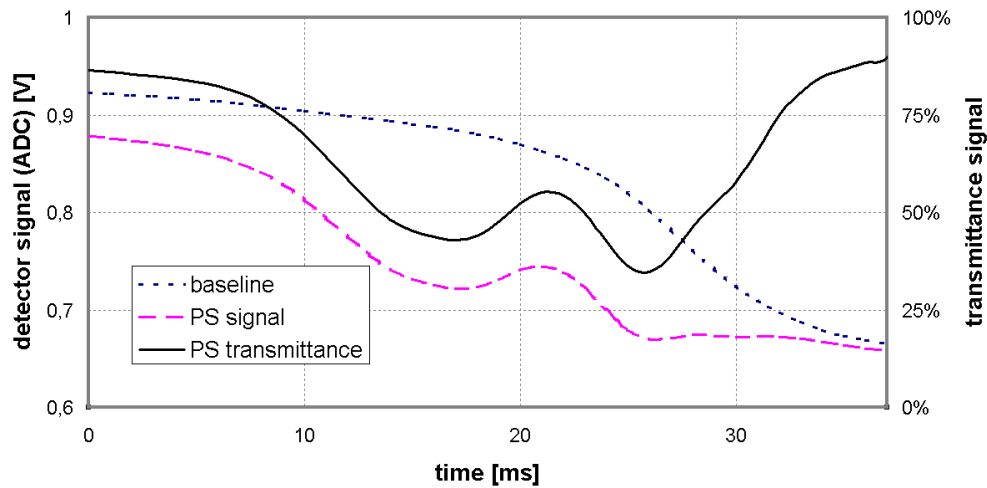


Fig 16: Fast sweep measurement example; PS foil
InAs Detector (Judson J12TE2) -30°C , IR-source IonOptics Reflect-IR 2,2W DC

The spectral resolution of the system deteriorates with increasing tuning rates because of the relatively low bandwidth of the pyroelectric detector. In applications where spectral resolution and speed are both of importance the usage of a fast photodiode might be required. We made measurements with a stand-alone FPF in a transmission package and an Indium Arsenide Detector to investigate the potential of such a configuration. Figure 16 shows the transmission measurement of a polystyrene foil. The transmittance signal is calculated by offset subtraction and division of sample and baseline signal. In comparison with the measured spectrum in Fig.13 one can see, that this measurement contains also all spectral information but can be performed in less than 50ms. Due to the dynamic nonlinearities of the FPF the filter tuning is not ideal linear. This causes a certain distortion of the spectrum along the time axis, which might be compensated by a better adapted voltage actuation or by software.

Evaluation Kit

As from now InfraTec offers an evaluation kit for this kind of devices. The kit should support customer needs for an initial test of the Fabry-Perot detectors without having to develop test circuitry and software themselves. It allows easy control of detector and IR source with customized software to analyze the detector signals. With the help of this kit a quick and easy configuration of a simple FP spectrometer is possible.

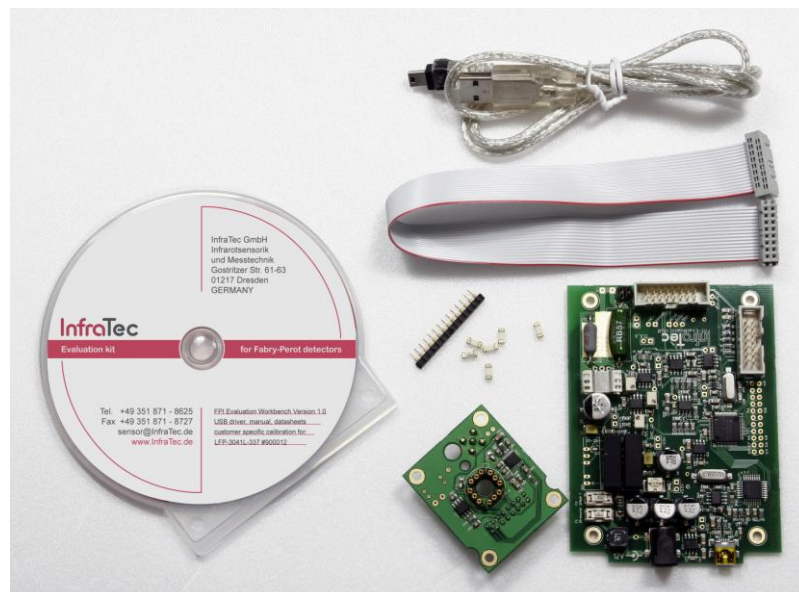


Fig 17: Evaluation Kit for FP detectors

Electronics and software of the Fabry-Perot evaluation kit are designed to give the user full access to performance and tuning capabilities of the Fabry-Perot detectors.

The basic operation principles are very similar as normally applied for conventional single or multicolor pyroelectric detectors: Modulation frequency, duty cycle and driving current of the IR source can be configured by software. The detector signal can be displayed real-time and recorded with 12 bit resolution and 1 kHz sampling frequency. Evaluation of the RMS amplitude is implemented by a FFT algorithm.

In addition to that, the electronics can provide voltages up to 35 V with 12 bit resolution to control the tunable filter. To easily create calibration files for the tuning, characteristics of individual detectors are also supported by the software. Latency for filter settling between measurements at different wavelengths can be configured, too.

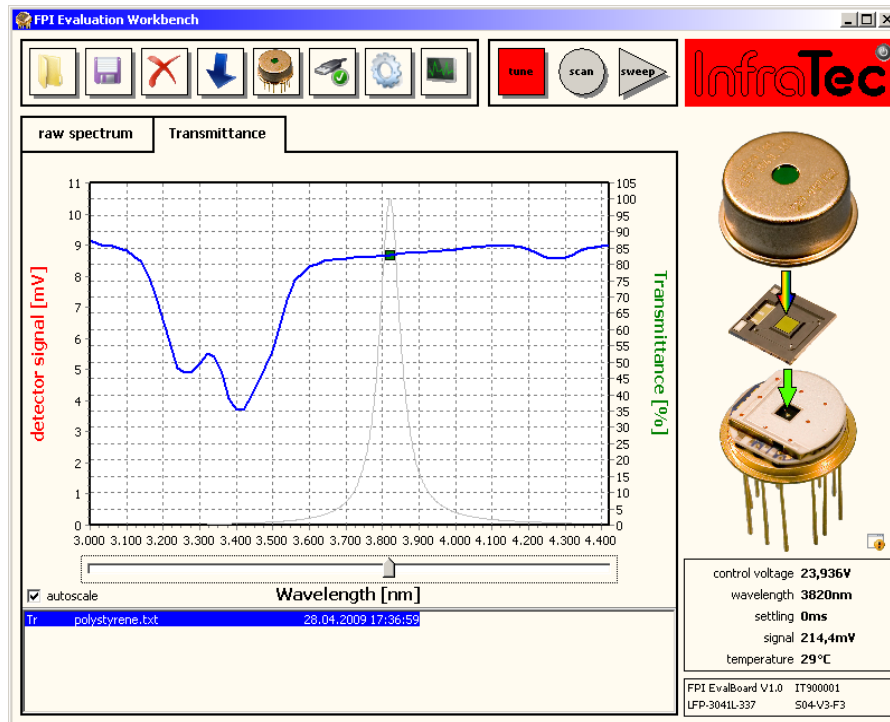


Fig 18: User interface of the evaluation software; Transmittance spectrum of a polystyrene foil measured in scan mode

In the basic operation mode the filter can be manually set to any wavelength within the tuning range. Measurements can continuously be recorded into a log file.

The more advanced Sequence mode is intended to compare the tunable detector with conventional multispectral solutions like filter wheels or multicolor detectors. The filter is periodically adjusted to a set of wavelengths, which can be predefined by the user.

The Scan mode is used to obtain complete spectra with a designated spectral range and step size. Measurements can be displayed and saved as raw signal spectra or as transmittance spectra if a previously measured background spectrum was defined as reference. An example of a scan measurement is shown in figure 18.

The software also supports the new innovative continuous sweep mode as described in this paper in the previous chapter. With the assistance of the software waveform, tuning speed and wavelength range can be adapted to find the most suitable operation. Recordings can be made with the integrated logging function, so external software can be used for further signal analysis.

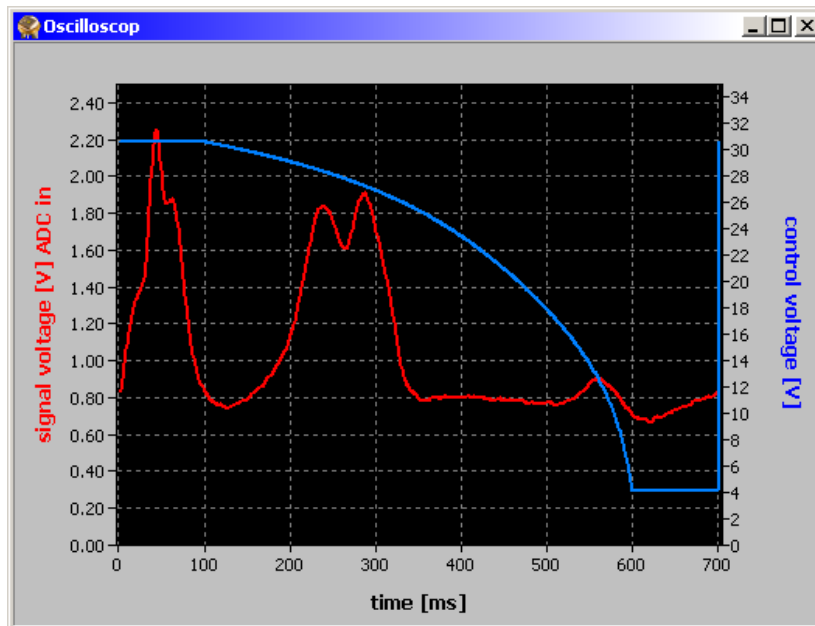


Fig 19: Sweep mode measurement of a polystyrene foil; detector signal and control voltage

Summary

The tunable infrared detector is based on a bulk micromachined spectrally tunable Fabry-Perot interferometer with an air cavity, which is electrostatically tuned and combined with a pyroelectric infrared detector. This ensures low cost, small size and high optical performance. We demonstrated the flexible use of the tunable detector in gas analyzers and spectroscopic applications. According to the optical setup and the operation mode high signal-to-noise-ratios of up to 8000:1 and spectral resolution $\lambda/\Delta\lambda$ of up to 75 were achieved. Continuously sweeping the Fabry-Perot filter opens up new capabilities of a pyroelectric detector. This particular operation mode has principally the potential to accelerate the recordings of spectra remarkably. New application fields include medical diagnostics and detection of hazardous substances in industrial and security environments.

References

- [1] S.H. Kong, D.D.L. Wijngaards, R.F. Wolffenbuttel, "Infrared micro-spectrometer based on a diffraction grating", *Sens. Actuators, A* 92-1, 88-95, (2001)
- [2] T. Sandner, H. Schenk, H. Lakner, A. Kenda, W. Scherf, „Einsatz translatorischer MOEMS-Aktoren für FTIR-Spektrometer“ *Proc. MikroSystemTechnik KONGRESS 2007*, VDE-Verlag, 2007, 485-488
- [3] D. Rossberg, "Silicon micromachined infrared sensor with tunable wavelength selectivity for application in infrared spectroscopy", *Sens. Actuators, A* 47, 413-416, (1995)
- [4] M. Noro, K. Suzuki, N. Kishi, H. Hara, T. Watanabe, and H. Iwaoko, "CO₂/H₂O gas sensor using tunable Fabry-Perot filter with wide wavelength range", *Proc. IEEE MEMS 2003 Conf.*, 319-322 (2003)
- [5] J.H. Jerman, D.J. Clift and S.R. Mallinson, "A miniature Fabry-Perot interferometer with corrugated silicon diaphragm support", *Sensors and Actuators A*, 29, 151-158 (1991).
- [6] N. Neumann, M. Ebermann, Kurth, K. Hiller, S., "Tunable infrared detector with integrated micromachined Fabry-Perot filter", *J.Micro/Nanolith. MEMS MOEMS* 7(2), 021004-01 - 021004-9 (2008)
- [7] H.A. Macleod, *Thin-Film optical filters*, IoP, Bristol and Philadelphia, 2001.
- [8] H. K. Lee, K. S. Kim, I. J. Cho, and E. Yoon, "A wide range linearly-tunable optical filter using magnetic actuation", *Proc. MEMS 2004*, 93-96 (2004)
- [9] H. Günzler, H.-U. Gremlich, *IR-Spektroskopie*, Wiley-VCH, Weinheim, 2003
- [10] Application note "Basics and Application of Variable Color Products"; *InfraTec Catalog* 2009